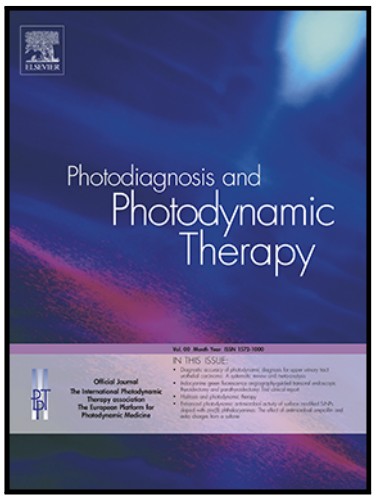

Current research status of Raman spectroscopy in glioma detection

Jie Liu , Pan Wang , Hua Zhang , Yuansen Guo , Mingjie Tang , Junwei Wang , Nan Wu

PII: S1572-1000(24)00425-3
DOI: https://doi.org/10.1016/j.pdpdt.2024.104388
Reference: PDPDT 104388

To appear in: *Photodiagnosis and Photodynamic Therapy*

Received date: 11 August 2024
Revised date: 5 October 2024
Accepted date: 18 October 2024

Please cite this article as: Jie Liu , Pan Wang , Hua Zhang , Yuansen Guo , Mingjie Tang , Junwei Wang , Nan Wu , Current research status of Raman spectroscopy in glioma detection, *Photodiagnosis and Photodynamic Therapy* (2024), doi: https://doi.org/10.1016/j.pdpdt.2024.104388

Highlights

- Raman spectroscopy enables a rapid, accurate, and label-free approach to glioma detection.
- Introduced the applications of Raman spectroscopy in glioma identification and classification.
- Discussed the main challenges in the clinical application of Raman spectroscopy.
- The article could provide some references for the further development of Raman spectroscopy in glioma diagnosis.

Current research status of Raman spectroscopy in glioma detection

Jie Liu [a, b], Pan Wang [a, b], Hua Zhang [c], Yuansen Guo [c], Mingjie Tang [c], Junwei Wang [a, b], Nan Wu [a, b, *]

[a] Department of Neurosurgery, Chongqing General Hospital, Chongqing University, Chongqing, 401147, China

[b] Chongqing Research Center for Glioma Precision Medicine, Chongqing University, Chongqing, 401147, China

[c] Chongqing Institute of Green and Intelligent Technology, Chongqing University, Chongqing, 400714, China

[*] Corresponding author: NO.118, Xingguang Avenue, Liangjiang New Aera, Chongqing, 401147, China. E-mail address: wunan881@tmmu.edu.cn (N. Wu).

Abstract:

Glioma is the most common primary tumor of the nervous system. Conventional diagnostic methods for glioma often involve time-consuming or reliance on externally introduced materials. Consequently, there is an urgent need for rapid and reliable diagnostic techniques. Raman spectroscopy has emerged as a promising tool, offering rapid, accurate, and label-free analysis with high sensitivity and specificity in biomedical applications. In this review, the fundamental principles of Raman spectroscopy have been introduced, and then the progress of applying Raman spectroscopy in biomedical studies has been summarized, including the identification and typing of glioma. The challenges encountered in the clinical application of Raman spectroscopy for glioma have been discussed, and the prospects have also been envisioned.

Keywords: Raman spectroscopy; Glioma detection; Histological typing; Molecular typing

1. Introduction

Glioma is the most common primary brain tumor arising from abnormal proliferation of glial cells, accounting for 30% of all brain tumors and 80% of all malignant brain tumors [1]. Patients with glioma suffered from low survival rates, with only 5.6% of glioblastoma patients surviving five years after diagnosis [2, 3]. Accurate diagnosis of glioma is crucial for prolonging the overall survival. Although histopathological methods such as hematoxylin-eosin [4] and immunohistochemical staining [5], along with advanced imaging methods such as computed tomography [6], magnetic resonance imaging [7], and positron emission tomography [8], are used to diagnose glioma and explore its mechanisms, these methods are often labor-intensive, time-consuming, and reliant on externally introduced materials [9]. Consequently, researchers are dedicated to developing new rapid and accurate methods for glioma detection.

Raman spectroscopic technique is a rapid, accurate, and label-free technique that is widely used in various fields [10, 11]. In the biomedical field, its rapid and accurate characteristics make it ideal for disease detection, and its label-free nature

demonstrates the potential for in vivo detection. During disease progression, substantial changes in the chemical compositions and structural characteristics promote tumor growth. Considerable details regarding the chemical compositions and structural characteristics are provided by Raman spectroscopy, which is thus able to detect changes during the onset and progression of disease [12, 13]. Over the past few decades, researchers have explored applications of Raman spectroscopy in tumor detection [14, 15], tumor imaging [16, 17], and tumor typing [18, 19] for glioma. These efforts have shown that Raman technology is a promising tool for glioma detection.

In this review, we introduced the fundamental principles of Raman spectroscopy, and then presented the applications of Raman spectroscopy in biomedical studies, including glioma identification and typing. Discussed the challenges encountered in the clinical application of Raman spectroscopy for glioma, and also explored the future prospects.

2. Raman spectroscopy techniques

Scattering phenomena occur across a broad spectrum, encompassing ultraviolet, visible, and near-infrared regions. When monochromatic radiation interacts with a substance, most photons are spontaneously scattered or dispersed at the same wavelength as the incident light, this process is known as elastic scattering [20]. In contrast, a small number of photons undergo inelastic scattering or Raman scattering, resulting in scattered photons with different wavelengths than the incident light [20]. Scattering phenomena involve the interaction of a photon with a molecule, resulting in a transition of the molecule's vibrational energy state. This energy exchange can lead to the emission of photons at different frequencies, categorized as Stokes and anti-Stokes Raman scattering [21, 22]. Stokes Raman scattering involves photons with frequencies lower than the incident light, while anti-Stokes Raman scattering involves photons with higher frequencies. The variation in photon frequency arises from energy exchange with the material, which is closely related to its molecular composition and structural properties. Notably, Raman scattering differs from infrared absorption, even though both processes involve transitions between vibrational energy states. The different scattering types and energy variations are shown in Fig. 1a.

Initially, Raman spectroscopy exhibited weak signals and low signal-to-noise ratios, which severely limited its applications [23, 24]. With the in-depth study of spectral theory by scientists and the rapid development of instruments, several novel Raman spectroscopy techniques have emerged. Those include surface-enhanced Raman spectroscopy [25, 26], micro-confocal Raman spectroscopy [27, 28], Coherent anti-Stokes Raman spectroscopy [21, 29], stimulated Raman spectroscopy [22, 30], and resonance Raman spectroscopy [31, 32]. These techniques have significantly improved the signal-to-noise ratio, reduced fluorescence interference, provided high-resolution images, and offered spatial information [33-35]. As a result, Raman spectroscopy has broader applications in biomedicine. The workflow for Raman spectroscopy collection is shown in Fig.1b. Peak assignment of biological samples was provided in Table 1 [44, 46, 48-53].

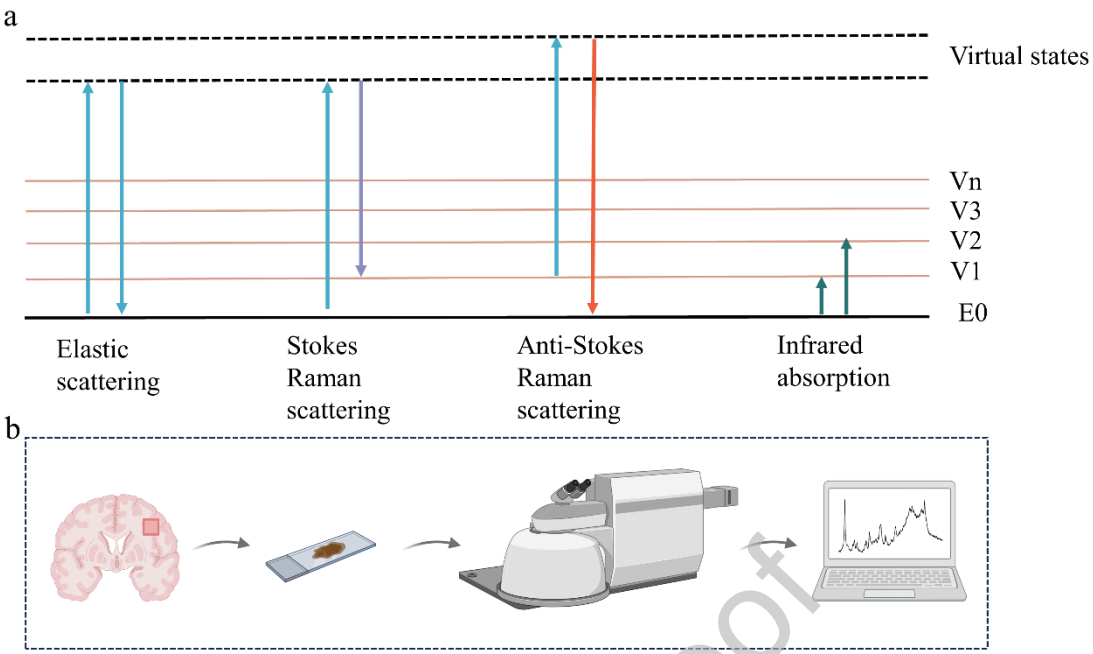

Fig. 1. (a) The different scattering types of elastic scattering, Raman scattering, and infrared absorption. Raman scattering is an inelastic process in which energy is exchanged between the incident photon and the vibrational states of the material, leading to the shifted frequencies of photons. (b) The workflow on Raman spectroscopy collection. Obtain tissue slices from brain surgery, collect information through Raman spectroscopy, transfer it to a computer, and map a Raman spectrum. Created with BioRender.com.

Table 1. Peak assignment of biological samples

Raman shift(cm^{-1})	Assignment
425	cholesterol
450	ring torsion of phenyl
474	glycogen and polysaccharides
498	nucleic acids, characteristic for DNA
547	cholesterol
596	phosphatidylinositol
612	cholesterol
620	C−C twist aromatic ring
624	phenylalanine
640	C−S stretching of cystine
642	C−C twisting mode of tyrosine
683	nucleic acids, characteristic of DNA
700	C−O stretching
719	C−N+ stretching of choline
727	nucleic acids, characteristic of DNA
757	protein, hemoglobin
782	DNA or RNA
825	phosphodiester
829	tyrosine
852	C−C stretching of tyrosine, collagen

857	protein, collagen
877	cholesterol
893	phosphodiesters
925	C−C bonds of the peptide backbone
933	proline, hydroxyproline
936	C−C stretching of Proline, valine, collagen
941	glycogen
961	cholesterol
968	lipids
1003	C−C phenylalanine ring breathing mode
1031	phenylalanine
1062	O−P−O stretch DNA
1081	lipids
1086	nucleic acid
1097	nucleic acid
1127	cytochrome c
1129	fatty acids
1159	carotenoids
1174	nucleic acid
1208	phenylalanine
1225	hemoglobin
1247	amide III
1250	nucleic acid
1269	amide II and III
1296	cholesterol and phospholipids
1313	lipids, collagen
1340	Tryptophan, nucleic acids
1370	nucleic acid
1397	lipids
1404	melanin
1439	proteins and lipids
1447	aliphatic amino acids
1486	nucleic acids
1523	carotenoids
1546	oxygenated hemoglobin
1578	nucleic acid
1585	hemoglobin
1596	melanin
1603	cytosine, phenylalanine and tyrosine
1614	aromatic amino acids
1616	C−C stretching of tyrosine and tryptophan
1623	hemoglobin
1657	lipids
1660	protein and lipids
1661	amide II and III
1667	amide
1735	cholesterol

3. Identification of glioma

The identification of glioma from normal brain tissue is important and is a prerequisite for the accurate outlining of glioma boundaries. Accurate delineation of glioma boundaries is critical in guiding surgeons to achieve precise resection, thereby reducing the recurrence rate of gliomas. Surgical resection is the first step in the multimodal treatment of gliomas, aimed at maximizing safe resection [36, 37]. The boundaries of surgical resection are determined by preoperative cranial magnetic resonance imaging and intraoperative microscopy. These methods offer an initial estimate of the glioma boundary. When faced with challenges in defining the tumor boundary, surgeons may resort to obtaining small tissue samples for rapid frozen pathological examination Based on the examination results, the surgeons can then accurately define the tumor boundary and subsequently remove the remaining tumor [38, 39]. Despite their limitations, these methods have become the optimal and most widely adopted method in current medical practice.

Raman spectroscopy has emerged as a powerful tool for probing molecular differences between tissues, aiding in the precise removal of gliomas by clearly defining their boundaries. It is well-established that biomolecular content and structure differ between glioma and normal brain tissues [15, 40, 41]. Recent studies have utilized Raman spectroscopy to demonstrate those differences at the cellular level, including in nucleic acids, proteins, and lipids [42, 43]. Mizuno et al. identified distinct molecular vibrational fingerprints at 1664 cm^{-1} (amide I), 1442 cm^{-1} (CH2 deformation), 2885 cm^{-1} (CH2 asymmetric stretching), and 2938 cm^{-1} (CH3 symmetric stretching) [44]. Similarly, Zhou et al. revealed significant peaks at 1157 cm^{-1}(carotenoids), 1521 cm^{-1} (carotenoids), 1588 cm^{-1} (tryptophan), 1640 cm^{-1} (amide I), 1550 cm^{-1} (amide II), 1306 cm^{-1} (amide III), 2934 cm^{-1} (protein), and 2885 cm^{-1} (lipid) [45]. Additionally, Kast et al. identified peaks at 985 cm^{-1} (calcifications), 1250 cm^{-1}(hemoglobin), 1159 cm^{-1} (carotenoids), 1585 cm^{-1} (hemoglobin), 1523 cm^{-1} (carotenoids), and 1739 cm^{-1} (cholesterol) [46]. These findings highlight the potential of Raman spectroscopy to effectively delineate glioma boundaries.

Peak intensities and peak ratios in Raman spectroscopy also reveal differences between glioma and normal tissue [47-49]. Ji et al. quantified tissue cell density, axon density, and protein: lipid ratios in gliomas and normal tissues, and found that the cell density and axon density of glioma were increased in gliomas, while protein: lipid ratios of glioma were decreased in gliomas [50]. Similarly, Lu et al. observed that cell density was highest in glioblastomas, intermediate in grade III gliomas, and lowest in normal brain tissue [51]. Additionally, Vrazhnov et al. noted an increase in lactate, tryptophan, fatty acids, and lipids in the mouse brain [52]. Iturrioz-Rodríguez et al. highlighted that the proliferation rate and mitochondrial content were increased in cancer cells, which was related to DNA/RNA and cytochrome c [47]. This increase in cell density and biomolecules during the development of glioblastoma can be detected by Raman spectroscopy imaging, which can distinguish between tumor and peripheral tissue based on differences in peak intensity and ratios. As shown in Figure 2, a clear boundary can be observed between the tumor and the peripheral tissue, highlighting distinct morphological characteristics between viable tumor tissue and necrosis.

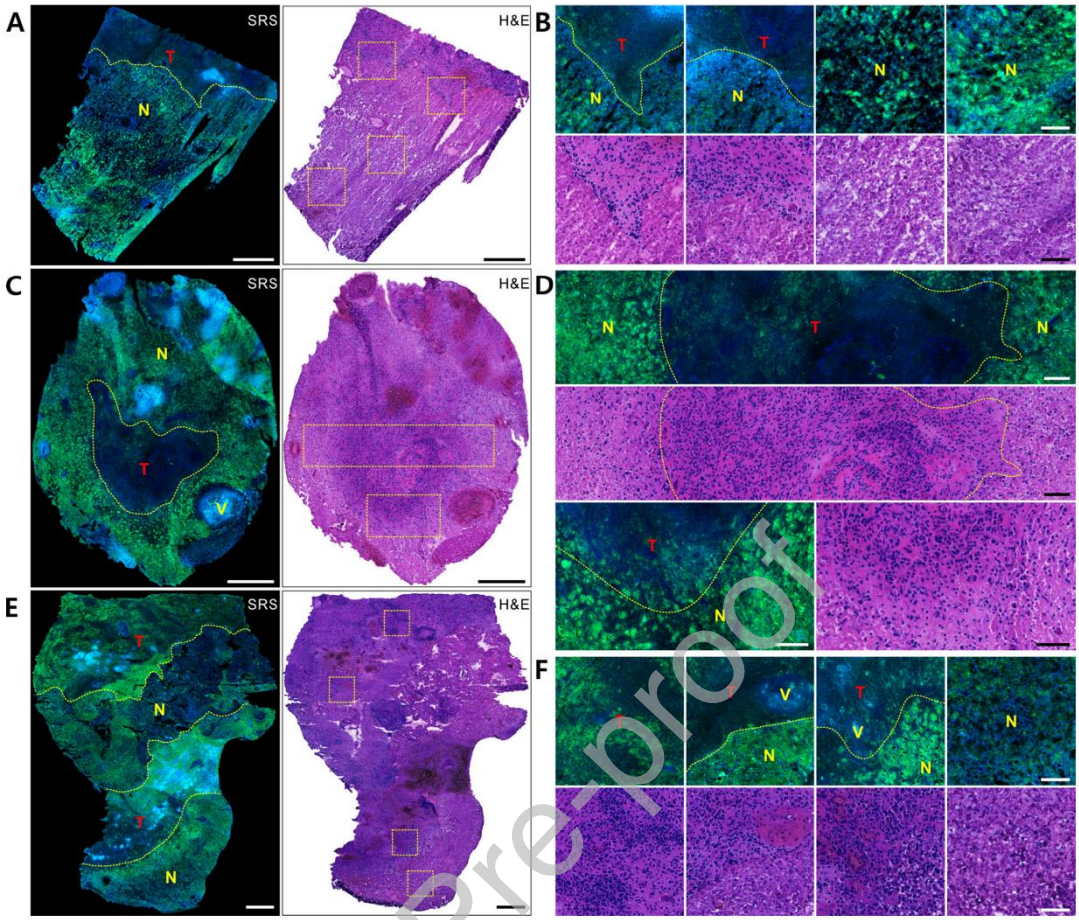

Fig. 2, Paired SRS and H&E staining imaging from the glioblastoma tissue boundaries. (A) Few tumors (labeled with T) and large areas of necrosis (labeled with N). (B) Central tumor and large peripheral area of necrosis. (C) Mixed distribution of tumor and necrosis. (B, D, F) showed zoom images of (A, C, E), respectively. Scale bars: (A, C, E), 500 μm; (B, D, F), 100 μm. Images reproduced with permission from Ref [51].

To rapidly delineate the boundaries of glioma, Raman spectroscopy is applied to fresh, unprocessed samples, aiding in precise surgical resection [31, 53-56]. Traditional methods such as complete immunohistochemical staining examination of glioma typically take more than one week and lack intraoperative guidance. Although rapid frozen histological examination can provide a quick diagnosis in about fifteen minutes, it is often less accurate. In contrast, Raman spectroscopy quickly detects glioma boundaries. Orringer et al. utilized stimulated Raman histology to map Raman shifts (2845 cm^{-1} and 2930 cm^{-1}) in fresh, unstained specimens from 101 neurosurgical patients, revealing cellular and structural features (cell density, vascular pattern, and nuclear structure) akin to H&E staining [57]. Hollon et al. proposed a new parallel workflow that combines stimulated Raman histology with deep convolutional neural networks, significantly reducing testing time for fresh samples. This workflow also achieves higher accuracy compared to traditional histopathological examination (94.6% vs. 93.9%) [58]. Di et al. studied 21 glioma

cases using stimulated Raman imaging, revealing a significant reduction in detection time compared to frozen sections (9.7 vs. 43 minutes) [59]. Therefore, utilizing fresh, unprocessed samples enables rapid and precise delineation of glioma boundaries.

4. Typing of glioma

4.1 Histological typing

Histological typing is crucial for the diagnosis and treatment of glioma. According to the 2021 World Health Organization classified central nervous system tumors, glioma can be categorized into adult-type diffuse glioma, pediatric-type diffuse low-grade glioma, pediatric-type diffuse high-grade glioma, circumscribed astrocytic glioma, and ependymal tumors [60]. Each category exhibits distinct prognoses and survival rates. Recent studies have increasingly focused on utilizing Raman spectroscopy to explore the histological features of glioma [61-63]. Ospanov et al. demonstrated differences in the histologic features among Raman spectra of glioblastoma, oligodendroglioma, and astrocytoma, using Raman spectroscopy combined with clustering and dimensionality reduction algorithms for differentiation [64]. The principal components of the Raman spectra were primarily influenced by phenylalanine, proteins, hemoglobin, lipids, and cholesterol. Hollon et al. analyzed 33 cases of brain tumors to identify key histologic features using stimulated Raman histology [65]. Pilocytic astrocytoma (grade I) exhibited unique hair-like protrusions, ganglioma presented giant neoplastic ganglion-like cells, and diffuse midline glioma (grade IV), displayed dysplasia and microvascular proliferation. Quesnel et al. developed a glycosylation database covering glucose, fucose, galactosamine, galactose, glucosamine, mannose, and neuraminic acid, and the accuracy of glioma grades was 80% (II vs III), 85% (III vs IV), and 75% (II vs IV), separately [66]. Li et al. established a surface-enhanced Raman scattering with an enhancement factor of up to 1.37×10^9 using silver nanoparticles modified silver nanorods as substrates [67]. They successfully differentiated glioma grades II, III, and IV using Raman spectra combined with principal component analysis. The accuracy of the classification ranged from 75 to 100% [28, 63, 65, 66, 68, 69]. Therefore, the precise differentiation of glioma grades and subtypes using Raman spectroscopy could serve as a stepping stone toward high-precision neurosurgery. Figure 3 illustrates the unique histologic features of glioma, including hypercellularity, nuclear atypia, microvascular proliferation, axonal disruption, and perineuronal satellitosis.

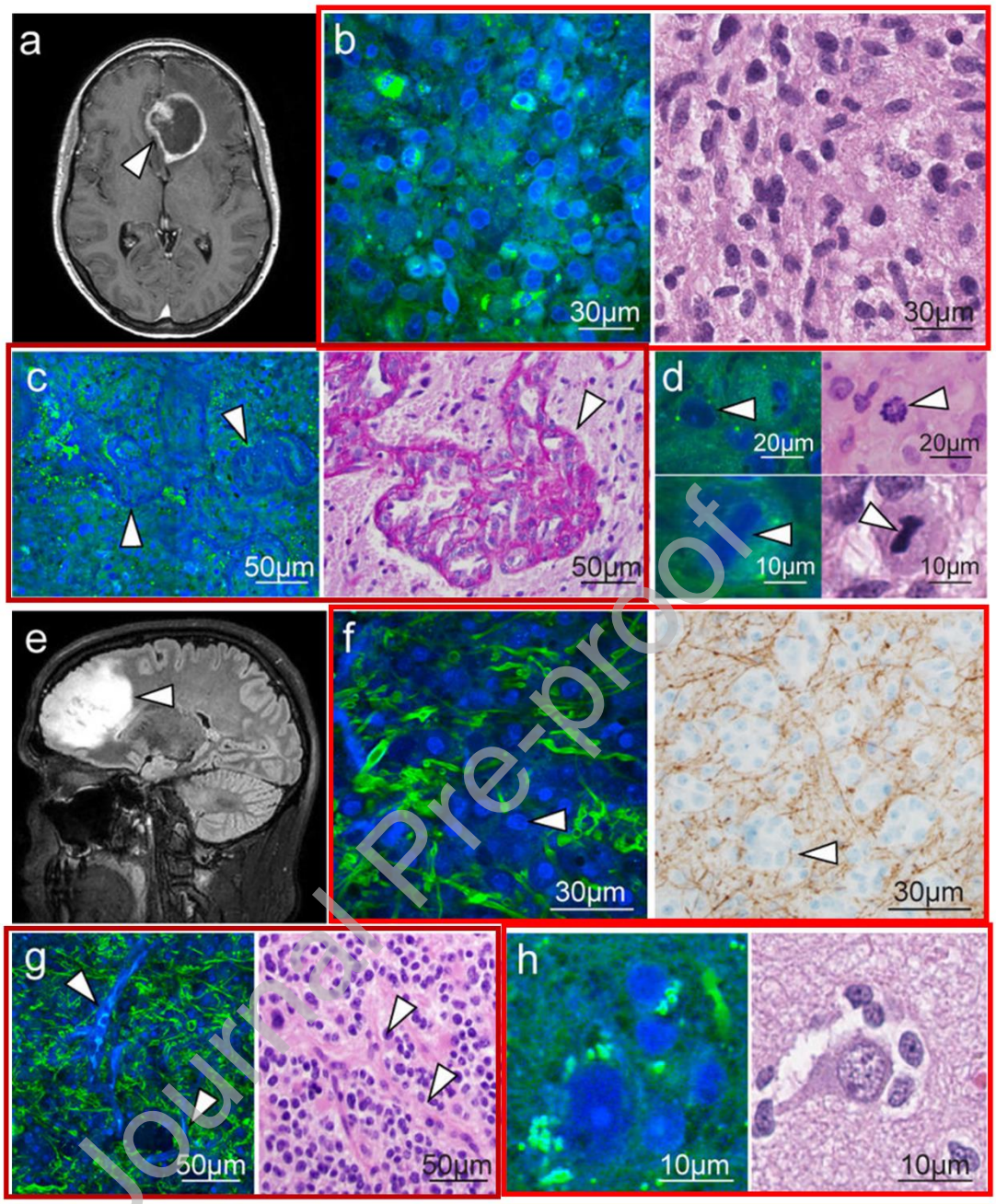

Fig. 3. MRI-based paired SRS and H&E staining imaging. (A) Glioblastoma shows ring enhancement on MRI. (B) Cellular proliferation and nuclear atypia of the live tumor are evident in both SRS (left) and H&E (right) staining. (C) Microvascular proliferation forms twisted vascular complexes (arrowheads). (D) Images of mitosis (arrowheads). (E) Low-grade oligodendroglioma (arrowhead). (F) Axonal disruption (left), corresponding to neurofilament immunostaining (right). (G) "Chicken wire" blood vessels (arrowheads). (H) Perineuronal satellitosis is visible in SRS (left) and H&E staining (right). Images reproduced with permission from Ref [50].

To facilitate real-time intraoperative histologic assessment of glioma, a specially designed and optimized Raman spectroscopy with a probe system was developed for in vivo measurements, marking a significant advancement [70-73]. Desroches et al

reported the successful in vivo measurement of Raman spectra using a hand-held probe system in normal brain tissue, necrotic tissue, and tumor tissue. They collected a total of 70 spectra from 10 patients and achieved an accuracy of 87%, sensitivity of 84%, and specificity of 89% using a leave-one-out cross-validation approach with the Boosted Trees algorithm [74]. Similarly, Jermyn et al. developed a hand-held contact Raman spectroscopy probe system capable of distinguishing between normal brain, dense cancer, and normal brain invaded by cancer cells, with a sensitivity of 93% and a specificity of 91%. This probe can also detect previously undetectable diffuse invasive glioma cells at cellular resolution [73]. Han et al. further enhanced Raman scattering probe sensitivity, achieving a detection limit of 5.0 pM in aqueous solution [75]. This probe offers higher resolution than MRI for defining glioma boundaries, potentially reducing glioma recurrence rates. These advancements in hand-held probe Raman spectroscopy systems could offer a high signal-to-noise ratio, high resolution, high accuracy rate, high sensitivity rate, and high specificity rate, significantly enhancing surgical guidance and patient outcomes. As can be seen in Figure 4, the Raman spectroscopy system probe can be integrated with MRI localization and H&E staining images to accurately differentiate between tumor and normal brain tissues.

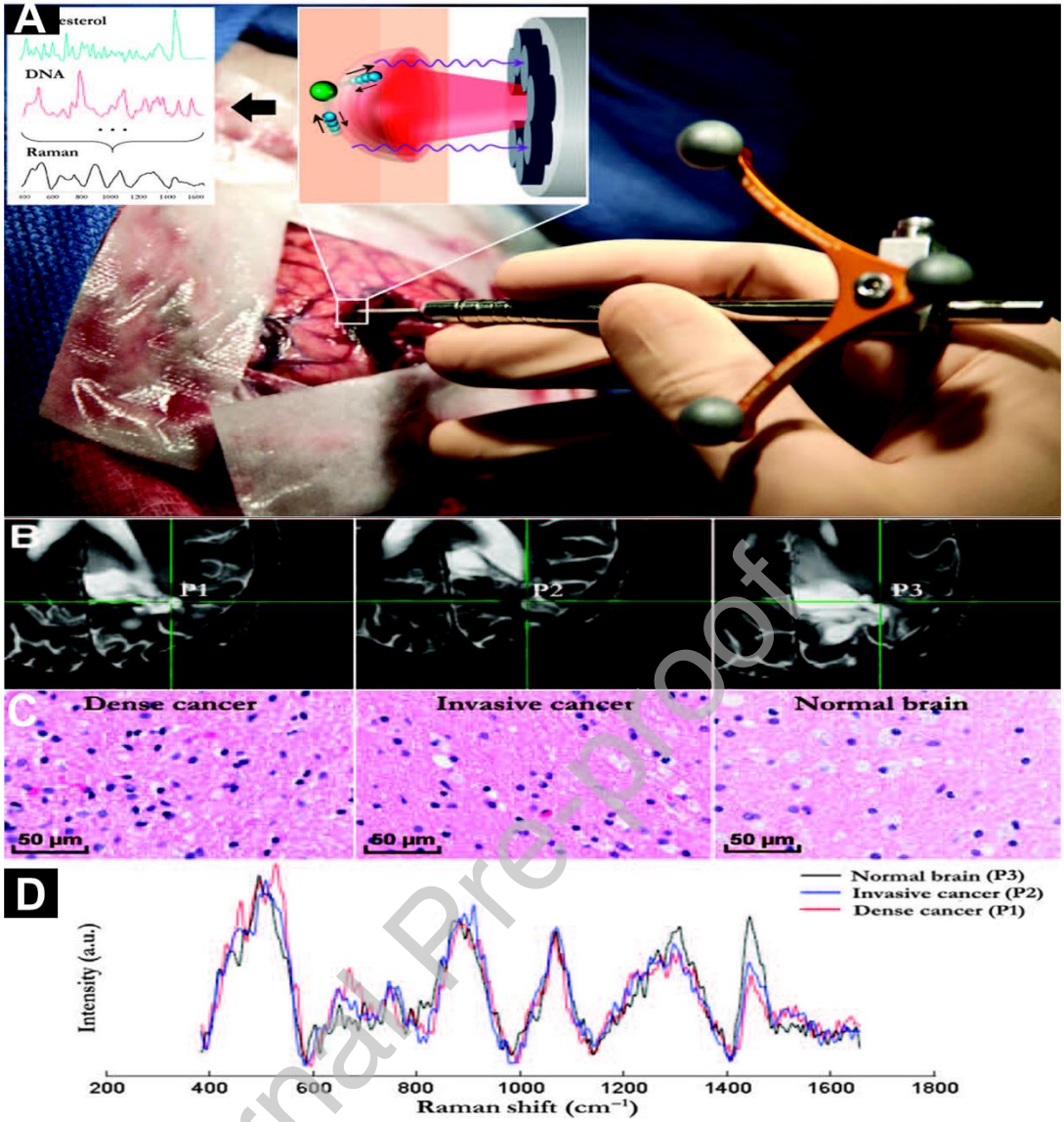

Fig. 4. Raman spectroscopy probe system for glioma detection. (A) Photograph of the hand-held contact Raman probe. (A) T2-weighted MRI images. (C) H&E staining images of dense cancer (P1), invasive cancer (P2), and normal brain (P3), corresponding to (B), respectively. (D) Raman spectroscopy image of tumor tissues with normal brain tissues. Images reproduced with permission from Ref [73].

Notably, Nicolson et al. demonstrated the first Raman imaging of gliomas in mice through intact skulls using surface-enhanced spatially offset resonance Raman spectroscopy, promising high precision in outlining glioma boundaries in vitro [63]. This study indicates the potential for seamless integration of Raman spectroscopy into the neurosurgical workflow. Consequently, this technique is expected to facilitate the detection of both glioma boundaries and histologic subtypes in vitro.

4.2 Molecular typing

Molecular typing is becoming increasingly vital for the diagnosis and treatment of glioma. In 2007, the World Health Organization classified central nervous system

tumors into main groups, which included astrocytic tumors, oligodendroglial tumors, oligoastrocytic tumors, ependymal tumors, and neuronal and mixed neuronal-glial tumors [76]. According to the 2016 World Health Organization criteria, the classification of glioma requires a combination of histologic features and molecular subtypes [77]. The 2021 World Health Organization criteria further emphasize the significance of molecular subtypes [60]. These molecular subtypes include isocitrate dehydrogenase (IDH) mutations, O6-methylguanine-DNA methyltransferase (MGMT) promoter methylation, chromosome 1p/19q deletion, telomerase reverse transcriptase (TERT) promoter mutations, epidermal growth factor receptor (EGFR) amplification, alpha thalassemia retardation syndrome X-linked (ATRX) mutations, TP53 mutations, and others [60]. Identifying these biologically and prognostically significant molecular subtypes has led to new categorizations of glioma [78, 79].

Spectral features of IDH-mutant glioma were investigated using Raman spectroscopy. The isocitrate dehydrogenase (IDH) family of enzymes catalyzes the conversion of isocitrate to α-ketoglutarate while converting nicotinamide adenine dinucleotide phosphate ($NADP^+$) to reduced $NADP^+$ (NADPH), both as part of the Kreb cycle and in the cytoplasm [80]. In glioma, most mutations are caused by amino acid substitutions from arginine to histidine at position 132 of IDH1 (R132H) and from arginine to lysine at position 172 of IDH2 (R172K) [81]. In adult patients, IDH mutations serve as positive prognostic markers with notable significance [82]. IDH-mutants are early changes in glioma formation and can be identified by Raman spectroscopy [48, 83, 84]. Uckermann et al. identified five Raman peaks at 498, 826, 1003, 1174, and 1337 cm^{-1} to differentiate between IDH1-mutant and IDH1-wildtype from 36 glioma cases, using Raman spectroscopy [85]. They revealed an increase in the intensity of the DNA bands and a significant decrease in the intensity of the lipid molecule bands in the Raman spectrum in IDH1-mutant gliomas. Livermore et al. used Raman spectroscopy to explore the spectral features peaks at 1445 cm^{-1} and 1660 cm^{-1} of IDH-mutant and IDH-wildtype from 62 fresh tissue samples. The most significant differences in peaks were found for lipids (853, 1059, 1087,1266, 1445, and 1660 cm^{-1}), phenylalanine (1003 cm^{-1}), and DNA (1207 and 1342 cm^{-1}). The classification model achieved a sensitivity of 0.91, a specificity of 0.95, and an accuracy of 0.98 [86]. Sciortino et al. used Raman spectroscopy to distinguish IDH-mutant from IDH-wildtype from 38 unprocessed samples. They demonstrated a decrease in the intensity of both the amide III peaks (1225, 1245, 1250, 1265, and 1275 cm^{-1}) and the heme blood (1454 cm-1) peaks in the IDH-mutant [87]. The Raman spectra of IDH-mutant indicated an increase in the intensity of peaks in DNA and proteins and a decrease in the intensity of peaks in lipids, amides, and heme. As can be seen in Figure 5, based on the spectral information acquired from glioma, the DeepGlioma predictions system can predict IDH mutations versus IDH-wildtype for molecular markers of gliomas, similar to the molecular subgroup heatmaps. Further research is warranted to expand the current understanding of distinguishing between IDH-mutant and IDH-wildtype, as existing literature on this topic remains limited.

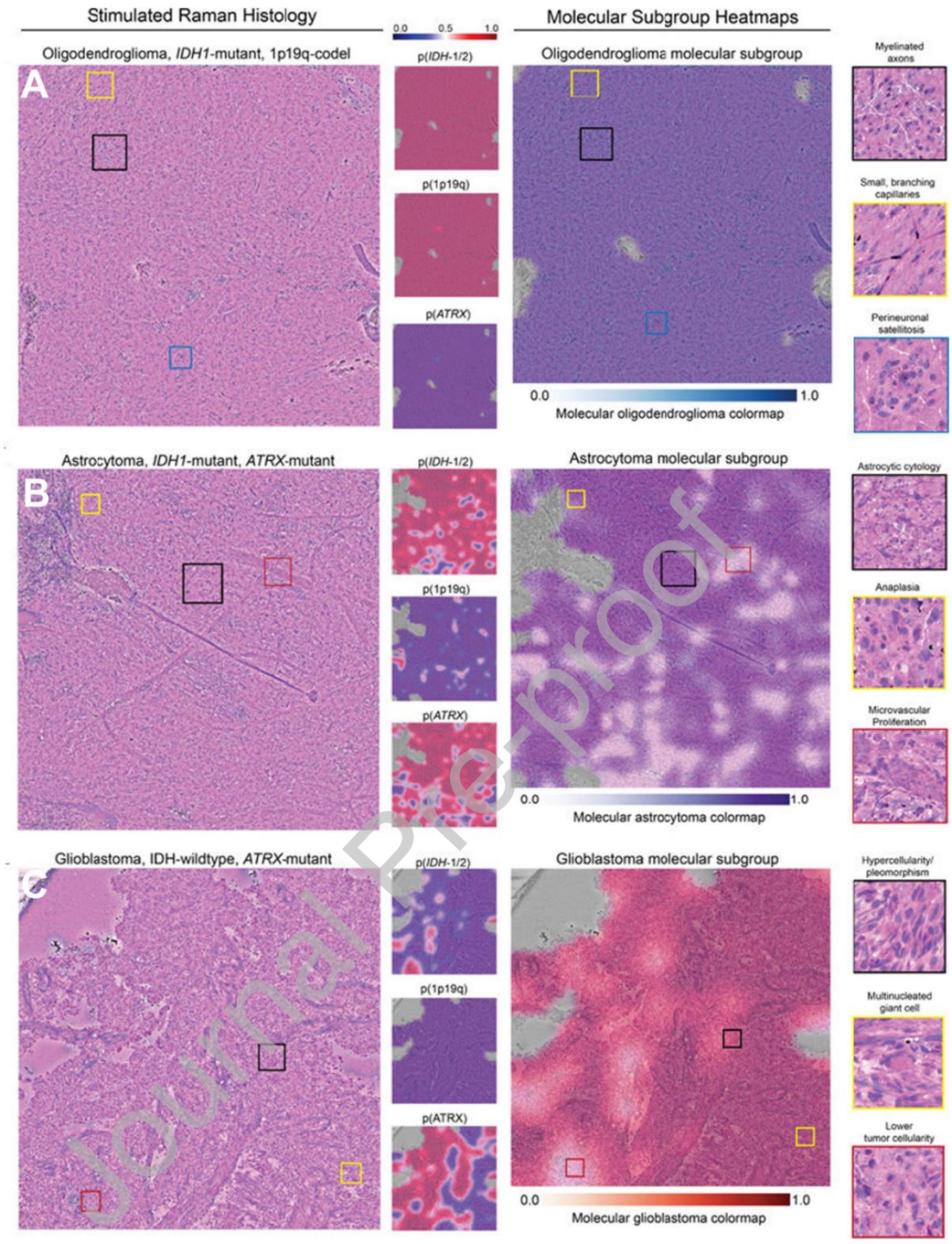

Fig. 5. Molecular marker and molecular subgroup heatmaps. (A) SRH image of a patient with molecular oligodendroglioma, IDH-mutant, 1p19q-codel. (B) SRH image of a patient with molecular astrocytoma, IDH-mutant, 1p19q-intact, and ARTX-mutation. (C) Glioblastoma, IDH-wildtype tumor. Images reproduced with permission from Ref [30].

Raman spectroscopy was employed to explore spectral features of MGMT promoter methylation in glioma. MGMT promoter methylation is frequently associated with IDH mutations. The DNA repair gene O6-methylguanine-DNA methyltransferase (MGMT) is the most significant epigenetically silenced gene in gliomas [88]. In glioma, MGMT repairs the most toxic damage caused by alkylating

agents O6-methylguanine, reflecting the fact that patients with an unmethylated MGMT do not benefit from concomitant and adjuvant radiotherapy with temozolomide [89, 90]. Higher levels of MGMT are thought to lead to temozolomide resistance and MGMT methylation status has become the first predictive biomarker in neuro-oncology [91]. Wang et al. utilized Raman spectroscopy to detect lipid droplets, i.e. triglycerides and cholesterol esters, in MGMT. Their findings indicated significantly lower levels in lipid droplets and cholesterol esters in MGMT unmethylated compared to MGMT methylated (MGMT methyl ≥15%) [92]. This study underscores the association between MGMT methylation and lipid accumulation in glioma, presenting potential avenues for diagnosing and treating temozolomide-resistant gliomas. Additional studies utilizing Raman spectroscopy are needed to clarify the correlation between clinical prognosis and MGMT promoter methylation.

Other molecular markers of glioma are also essential for treatment and prognosis [93-97]. Chromosome 1p/19q co-deletion has been known as a diagnostic and prognostic marker for oligodendroglioma [98, 99]. ATRX is a crucial component of a multiprotein complex containing death-associated protein 6 (DAXX) [100]. ATRX protein loss and ATRX gene mutations are genomically unstable and often found in astrocytomas, IDH mutant [101]. The TERT gene encodes the catalytic reverse transcriptase subunit of telomerase, which is essential for maintaining telomere length [102]. Approximately 70% of adult primary glioblastomas contain TERT promoter mutations [103]. TERT promoter mutations are a poor prognostic factor but occur predominantly in IDH wild-type gliomas [104]. However, there are no relevant studies utilizing Raman spectroscopy, which will be the focus and gap of future research.

5. Challenges and prospects

Raman spectroscopy, recognized for its rapid, accurate, and label-free characteristics, has emerged as a promising tool for detecting glioma. However, several challenges remain before it can be widely adopted in clinical practice.

First, detection workflows based on Raman spectroscopy vary considerably across studies. There is a lack of uniformity among different studies, including the setting of spectrometers, the acquisition of spectra, and the pre-processing of data [105-107]. This means that different protocols in different laboratories analyzing the same biological samples may have differences in the spectra. Therefore, establishing a unified and standardized workflow based on Raman spectroscopy is essential.

Second, detection programs for biological samples are different [108-110]. The selection of biological samples includes fresh tissue, frozen sections, and paraffin sections, depending on the specific goals of the study. Most studies utilize in vitro tissues, with only a few involving in vivo analyses. Key metrics such as accuracy, sensitivity, and specificity should be further considered in vitro detection. To fully support the use of Raman spectroscopy in clinical practice, additional large-scale clinical trials and multicenter studies in vivo are necessary to validate the quantitative and qualitative findings.

Third, the acquisition time of large-area spectral imaging takes a relatively long time. Although Raman spectroscopy techniques are generally considered rapid, acquiring large-area spectral images can be time-consuming. This is because typical spectra of biological samples require large-area imaging spectra from multiple locations. In vivo detection may further extend procedure times, potentially compromising patient safety. Therefore, clinical practice must carefully consider the balance between acquisition time and spectrum quality.

Last, the signal of Raman spectroscopy may affect both the spectroscopic devices and the biological tissue. Due to its inherently weak nature, the Raman signal can be easily interfered with by background noise from the measurement device or the tissue itself. Enhancing signal-to-noise ratios through adjustments to laser power or integration time is not suitable for in vivo detection. Patient safety is paramount, and it is crucial to avoid damage to normal brain tissue during detection, and rigorous safety testing must be conducted before implementing this technique in clinical practice.

In conclusion, glioma detection based on Raman spectroscopy has a promising application prospect. With the rapid development of modern technology and the continuous improvement in spectroscopic instruments, we have reason to believe that the above challenges of Raman spectroscopy will gradually be addressed. Raman spectroscopy provides a reliable method for the digital diagnosis and treatment of glioma, making a significant contribution to enhancing people's quality of life and overall health.

Acknowledgments

This work was supported by the Chongqing medical scientific research project (Joint project of Chongqing Health Commission and Science and Technology Bureau) (CSTC2021jscx-gksb-N0024) and (2023QNXM043).

Author contributions: CRediT

Jie Liu: Writing – original draft, Validation, Investigation, Formal analysis, Conceptualization.
Pan Wang: Methodology, Validation, Formal analysis.
Hua Zhang: Investigation, Validation, Visualization.
Yuansen Guo: Validation, Formal analysis.
Mingjie Tang: Visualization, Investigation, Formal analysis.
Junwei Wang: Conceptualization, Investigation, Formal analysis.
Nan Wu: Writing – review & editing, Conceptualization, Supervision, Resources, Project administration, Funding acquisition.

Declaration of competing interest

The authors declare that they have no known competing financial interests or personal relationships that could have appeared to influence the work reported in this paper.

Data availability

Data will be made available on request.

References

[1] M. Weller, W. Wick, K. Aldape, M. Brada, M. Berger, S.M. Pfister, R. Nishikawa, M. Rosenthal, P.Y. Wen, R. Stupp, G. Reifenberger, Glioma, Nature Reviews Disease Primers 1(1) (2015). https://doi.org/10.1038/nrdp.2015.17.

[2] C. Luo, S. Xu, G. Dai, Z. Xiao, L. Chen, Z. Liu, Tumor treating fields for high-grade gliomas, Biomed. Pharmacother. 127 (2020). https://doi.org/10.1016/j.biopha.2020.110193.

[3] J.T. Huse, K.D. Aldape, The Evolving Role of Molecular Markers in the Diagnosis and Management of Diffuse Glioma, Clin. Cancer Res. 20(22) (2014) 5601-5611. https://doi.org/10.1158/1078-0432.Ccr-14-0831.

[4] M. Weller, M. van den Bent, M. Preusser, E. Le Rhun, J.C. Tonn, G. Minniti, M. Bendszus, C. Balana, O. Chinot, L. Dirven, P. French, M.E. Hegi, A.S. Jakola, M. Platten, P. Roth, R. Rudà, S. Short, M. Smits, M.J.B. Taphoorn, A. von Deimling, M. Westphal, R. Soffietti, G. Reifenberger, W. Wick, EANO guidelines on the diagnosis and treatment of diffuse gliomas of adulthood, Nature Reviews Clinical Oncology 18(3) (2020) 170-186. https://doi.org/10.1038/s41571-020-00447-z.

[5] S. Lapointe, A. Perry, N.A. Butowski, Primary brain tumours in adults, The Lancet 392(10145) (2018) 432-446. https://doi.org/10.1016/s0140-6736(18)30990-5.

[6] M.J. van den Bent, M. Geurts, P.J. French, M. Smits, D. Capper, J.E.C. Bromberg, S.M. Chang, Primary brain tumours in adults, The Lancet 402(10412) (2023) 1564-1579. https://doi.org/10.1016/s0140-6736(23)01054-1.

[7] I. Mecheter, M. Abbod, A. Amira, H. Zaidi, Deep learning with multiresolution handcrafted features for brain MRI segmentation, Artif. Intell. Med. 131 (2022). https://doi.org/10.1016/j.artmed.2022.102365.

[8] K.-J. Langen, A. Heinzel, P. Lohmann, F.M. Mottaghy, N. Galldiks, Advantages and limitations of amino acid PET for tracking therapy response in glioma patients, Expert Rev. Neurother. 20(2) (2019) 137-146. https://doi.org/10.1080/14737175.2020.1704256.

[9] D. Sturm, D. Capper, F. Andreiuolo, M. Gessi, C. Kölsche, A. Reinhardt, P. Sievers, A.K. Wefers, A. Ebrahimi, A.K. Suwala, G.H. Gielen, M. Sill, D. Schrimpf, D. Stichel, V. Hovestadt, B. Daenekas, A. Rode, S. Hamelmann, C. Previti, N. Jäger, I. Buchhalter, M. Blattner-Johnson, B.C. Jones, M. Warmuth-Metz, B. Bison, K. Grund, C. Sutter, S. Hirsch, N. Dikow, M. Hasselblatt, U. Schüller, A. Koch, N.U. Gerber, C.L. White, M.K. Buntine, K. Kinross, E.M. Algar, J.R. Hansford, N.G. Gottardo, M.U. Schuhmann, U.W. Thomale, P. Hernáiz Driever, A. Gnekow, O. Witt, H.L. Müller, G. Calaminus, G. Fleischhack, U. Kordes, M. Mynarek, S. Rutkowski, M.C. Frühwald, C.M. Kramm, A. von Deimling, T. Pietsch, F. Sahm, S.M. Pfister, D.T.W. Jones, Multiomic neuropathology improves diagnostic accuracy in pediatric neuro-oncology, Nat. Med. 29(4) (2023) 917-926. https://doi.org/10.1038/s41591-023-02255-1.

[10] M. Vendrell, K.K. Maiti, K. Dhaliwal, Y.-T. Chang, Surface-enhanced Raman scattering in cancer detection and imaging, Trends Biotechnol. 31(4) (2013) 249-257. https://doi.org/10.1016/j.tibtech.2013.01.013.

[11] X. Zheng, C. Zong, M. Xu, X. Wang, B. Ren, Raman Imaging from Microscopy to Nanoscopy,

and to Macroscopy, Small 11(28) (2015) 3395-3406. https://doi.org/10.1002/smll.201403804.
[12] J. Liu, P. Wang, H. Zhang, N. Wu, Distinguishing brain tumors by Label-free confocal micro-Raman spectroscopy, Photodiagnosis and Photodynamic Therapy 45 (2024). https://doi.org/10.1016/j.pdpdt.2024.104010.
[13] H. Wang, J. Li, J. Qin, J. Li, Y. Chen, D. Song, H. Zeng, S. Wang, Confocal Raman microspectral analysis and imaging of the drug response of osteosarcoma to cisplatin, Anal. Methods 13(22) (2021) 2527-2536. https://doi.org/10.1039/d1ay00626f.
[14] H. Abramczyk, B. Brozek-Pluska, A. Jarota, J. Surmacki, A. Imiela, M. Kopec, A look into the use of Raman spectroscopy for brain and breast cancer diagnostics: linear and non-linear optics in cancer research as a gateway to tumor cell identity, Expert Rev. Mol. Diagn. 20(1) (2020) 99-115. https://doi.org/10.1080/14737159.2020.1724092.
[15] S.N. Kalkanis, R.E. Kast, M.L. Rosenblum, T. Mikkelsen, S.M. Yurgelevic, K.M. Nelson, A. Raghunathan, L.M. Poisson, G.W. Auner, Raman spectroscopy to distinguish grey matter, necrosis, and glioblastoma multiforme in frozen tissue sections, J. Neurooncol. 116(3) (2014) 477-485. https://doi.org/10.1007/s11060-013-1326-9.
[16] T. Hollon, D.A. Orringer, Label-free brain tumor imaging using Raman-based methods, J. Neurooncol. 151(3) (2021) 393-402. https://doi.org/10.1007/s11060-019-03380-z.
[17] L. Van Hese, S. De Vleeschouwer, T. Theys, S. Rex, R.M.A. Heeren, E. Cuypers, The diagnostic accuracy of intraoperative differentiation and delineation techniques in brain tumours, Discover Oncology 13(1) (2022). https://doi.org/10.1007/s12672-022-00585-z.
[18] Y. Zhang, H. Yu, Y. Li, H. Xu, L. Yang, P. Shan, Y. Du, X. Yan, X. Chen, Raman spectroscopy: A prospective intraoperative visualization technique for gliomas, Frontiers in Oncology 12 (2023). https://doi.org/10.3389/fonc.2022.1086643.
[19] S. Murugappan, S.A.M. Tofail, N.D. Thorat, Raman Spectroscopy: A Tool for Molecular Fingerprinting of Brain Cancer, ACS Omega 8(31) (2023) 27845-27861. https://doi.org/10.1021/acsomega.3c01848.
[20] C. Raman, K. Krishnan, A new type of secondary radiation, Nature 501–502 (1928).
[21] A.A. Fung, L. Shi, Mammalian cell and tissue imaging using Raman and coherent Raman microscopy, WIREs Systems Biology and Medicine 12(6) (2020). https://doi.org/10.1002/wsbm.1501.
[22] B. Sarri, R. Canonge, X. Audier, E. Simon, J. Wojak, F. Caillol, C. Cador, D. Marguet, F. Poizat, M. Giovannini, H. Rigneault, Fast stimulated Raman and second harmonic generation imaging for intraoperative gastro-intestinal cancer detection, Scientific Reports 9(1) (2019). https://doi.org/10.1038/s41598-019-46489-x.
[23] X.Y. Zhao, G.Y. Liu, Y.T. Sui, M. Xu, L. Tong, Denoising method for Raman spectra with low signal-to-noise ratio based on feature extraction, Spectrochimica Acta Part A: Molecular and Biomolecular Spectroscopy 250 (2021). https://doi.org/10.1016/j.saa.2020.119374.
[24] Z. Li, Z. Li, Q. Chen, J. Zhang, M.E. Dunham, A.J. McWhorter, J.-M. Feng, Y. Li, S. Yao, J. Xu, Machine-learning-assisted spontaneous Raman spectroscopy classification and feature extraction for the diagnosis of human laryngeal cancer, Comput. Biol. Med. 146 (2022). https://doi.org/10.1016/j.compbiomed.2022.105617.
[25] L. Wu, A. Dias, L. Dieguez, Surface enhanced Raman spectroscopy for tumor nucleic acid: Towards cancer diagnosis and precision medicine, Biosens. Bioelectron. 204 (2022) 114075. https://doi.org/10.1016/j.bios.2022.114075.

[26] L. Golubewa, R. Karpicz, I. Matulaitiene, A. Selskis, D. Rutkauskas, A. Pushkarchuk, T. Khlopina, D. Michels, D. Lyakhov, T. Kulahava, A. Shah, Y. Svirko, P. Kuzhir, Surface-Enhanced Raman Spectroscopy of Organic Molecules and Living Cells with Gold-Plated Black Silicon, ACS Appl. Mater. Interfaces 12(45) (2020) 50971-50984. https://doi.org/10.1021/acsami.0c13570.

[27] J. Wen, T. Tang, S. Kanwal, Y. Lu, C. Tao, L. Zheng, D. Zhang, Z. Gu, Detection and Classification of Multi-Type Cells by Using Confocal Raman Spectroscopy, Front Chem 9 (2021) 641670. https://doi.org/10.3389/fchem.2021.641670.

[28] L.M. Wurm, B. Fischer, V. Neuschmelting, D. Reinecke, I. Fischer, R.S. Croner, R. Goldbrunner, M.C. Hacker, J. Dybaś, U.D. Kahlert, Rapid, label-free classification of glioblastoma differentiation status combining confocal Raman spectroscopy and machine learning, The Analyst 148(23) (2023) 6109-6119. https://doi.org/10.1039/d3an01303k.

[29] K. Aljakouch, Z. Hilal, I. Daho, M. Schuler, S.D. Krauss, H.K. Yosef, J. Dierks, A. Mosig, K. Gerwert, S.F. El-Mashtoly, Fast and Noninvasive Diagnosis of Cervical Cancer by Coherent Anti-Stokes Raman Scattering, Anal. Chem. 91(21) (2019) 13900-13906. https://doi.org/10.1021/acs.analchem.9b03395.

[30] T. Hollon, C. Jiang, A. Chowdury, M. Nasir-Moin, A. Kondepudi, A. Aabedi, A. Adapa, W. Al-Holou, J. Heth, O. Sagher, P. Lowenstein, M. Castro, L.I. Wadiura, G. Widhalm, V. Neuschmelting, D. Reinecke, N. von Spreckelsen, M.S. Berger, S.L. Hervey-Jumper, J.G. Golfinos, M. Snuderl, S. Camelo-Piragua, C. Freudiger, H. Lee, D.A. Orringer, Artificial-intelligence-based molecular classification of diffuse gliomas using rapid, label-free optical imaging, Nat. Med. 29(4) (2023) 828-832. https://doi.org/10.1038/s41591-023-02252-4.

[31] V. Neuschmelting, S. Harmsen, N. Beziere, H. Lockau, H.T. Hsu, R. Huang, D. Razansky, V. Ntziachristos, M.F. Kircher, Dual-Modality Surface-Enhanced Resonance Raman Scattering and Multispectral Optoacoustic Tomography Nanoparticle Approach for Brain Tumor Delineation, Small 14(23) (2018). https://doi.org/10.1002/smll.201800740.

[32] E. Bendau, J. Smith, L. Zhang, E. Ackerstaff, N. Kruchevsky, B. Wu, J.A. Koutcher, R. Alfano, L. Shi, Distinguishing metastatic triple-negative breast cancer from nonmetastatic breast cancer using second harmonic generation imaging and resonance Raman spectroscopy, J. Biophotonics 13(7) (2020). https://doi.org/10.1002/jbio.202000005.

[33] L. Xiao, C. Wang, C. Dai, L.E. Littlepage, J. Li, Z.D. Schultz, Untargeted Tumor Metabolomics with Liquid Chromatography–Surface-Enhanced Raman Spectroscopy, Angewandte Chemie International Edition 59(9) (2020) 3439-3443. https://doi.org/10.1002/anie.201912387.

[34] J. Lin, M.E. Graziotto, P.A. Lay, E.J. New, A Bimodal Fluorescence-Raman Probe for Cellular Imaging, Cells 10(7) (2021). https://doi.org/10.3390/cells10071699.

[35] D. Franco, S. Trusso, E. Fazio, A. Allegra, C. Musolino, A. Speciale, F. Cimino, A. Saija, F. Neri, M.S. Nicolò, S.P.P. Guglielmino, Raman spectroscopy differentiates between sensitive and resistant multiple myeloma cell lines, Spectrochimica Acta Part A: Molecular and Biomolecular Spectroscopy 187 (2017) 15-22. https://doi.org/10.1016/j.saa.2017.06.020.

[36] R. Ma, M.J.B. Taphoorn, P. Plaha, Advances in the management of glioblastoma, J. Neurol. Neurosurg. Psychiatry 92(10) (2021) 1103-1111. https://doi.org/10.1136/jnnp-2020-325334.

[37] J.S. Young, R.A. Morshed, S.L. Hervey-Jumper, M.S. Berger, The surgical management of diffuse gliomas: Current state of neurosurgical management and future directions, Neuro-oncol. 25(12) (2023) 2117-2133. https://doi.org/10.1093/neuonc/noad133.

[38] M. Blokker, P.C.d.W. Hamer, P. Wesseling, M.L. Groot, M. Veta, Fast intraoperative histology-

based diagnosis of gliomas with third harmonic generation microscopy and deep learning, Scientific Reports 12(1) (2022). https://doi.org/10.1038/s41598-022-15423-z.

[39] F. Sahm, S. Brandner, L. Bertero, D. Capper, P.J. French, D. Figarella-Branger, F. Giangaspero, C. Haberler, M.E. Hegi, B.W. Kristensen, K.M. Kurian, M. Preusser, B.B.J. Tops, M. van den Bent, W. Wick, G. Reifenberger, P. Wesseling, Molecular diagnostic tools for the World Health Organization (WHO) 2021 classification of gliomas, glioneuronal and neuronal tumors; an EANO guideline, Neuro-oncol. 25(10) (2023) 1731-1749. https://doi.org/10.1093/neuonc/noad100.

[40] S. Teuber-Hanselmann, E. Meinl, A. Junker, MicroRNAs in gray and white matter multiple sclerosis lesions: impact on pathophysiology, The Journal of Pathology 250(5) (2020) 496-509. https://doi.org/10.1002/path.5399.

[41] M. Prins, E. Schul, J. Geurts, P. van der Valk, B. Drukarch, A.M. van Dam, Pathological differences between white and grey matter multiple sclerosis lesions, Ann. N. Y. Acad. Sci. 1351(1) (2015) 99-113. https://doi.org/10.1111/nyas.12841.

[42] J. Herta, A. Cho, T. Roetzer-Pejrimovsky, R. Höftberger, W. Marik, G. Kronreif, T. Peilnsteiner, K. Rössler, S. Wolfsberger, Optimizing maximum resection of glioblastoma: Raman spectroscopy versus 5-aminolevulinic acid, J. Neurosurg. (2022) 1-10. https://doi.org/10.3171/2022.11.Jns22693.

[43] J. Depciuch, B. Tolpa, P. Witek, K. Szmuc, E. Kaznowska, M. Osuchowski, P. Krol, J. Cebulski, Raman and FTIR spectroscopy in determining the chemical changes in healthy brain tissues and glioblastoma tumor tissues, Spectrochim. Acta. A. Mol. Biomol. Spectrosc. 225 (2020) 117526. https://doi.org/10.1016/j.saa.2019.117526.

[44] A. Mizuno, T. Hayashi, K. Tashibu, S. Maraishi, K. Kawauchi, Y. Ozaki, Near-infrared FT-Raman spectra of the rat brain tissues, Neurosci. Lett. 141(1) (1992) 47-52. https://doi.org/10.1016/0304-3940(92)90331-z.

[45] Y. Zhou, C.-H. Liu, B. Wu, X. Yu, G. Cheng, K. Zhu, K. Wang, C. Zhang, M. Zhao, R. Zong, L. Zhang, L. Shi, R.R. Alfano, Optical biopsy identification and grading of gliomas using label-free visible resonance Raman spectroscopy, J. Biomed. Opt. 24(09) (2019). https://doi.org/10.1117/1.Jbo.24.9.095001.

[46] R.E. Kast, G.W. Auner, M.L. Rosenblum, T. Mikkelsen, S.M. Yurgelevic, A. Raghunathan, L.M. Poisson, S.N. Kalkanis, Raman molecular imaging of brain frozen tissue sections, J. Neurooncol. 120(1) (2014) 55-62. https://doi.org/10.1007/s11060-014-1536-9.

[47] N. Iturrioz-Rodríguez, D. De Pasquale, P. Fiaschi, G. Ciofani, Discrimination of glioma patient-derived cells from healthy astrocytes by exploiting Raman spectroscopy, Spectrochimica Acta Part A: Molecular and Biomolecular Spectroscopy 269 (2022). https://doi.org/10.1016/j.saa.2021.120773.

[48] R. Galli, M. Meinhardt, E. Koch, G. Schackert, G. Steiner, M. Kirsch, O. Uckermann, Rapid Label-Free Analysis of Brain Tumor Biopsies by Near Infrared Raman and Fluorescence Spectroscopy-A Study of 209 Patients, Front Oncol 9 (2019) 1165. https://doi.org/10.3389/fonc.2019.01165.

[49] É. Lemoine, F. Dallaire, R. Yadav, R. Agarwal, S. Kadoury, D. Trudel, M.-C. Guiot, K. Petrecca, F. Leblond, Feature engineering applied to intraoperativein vivoRaman spectroscopy sheds light on molecular processes in brain cancer: a retrospective study of 65 patients, The Analyst 144(22) (2019) 6517-6532. https://doi.org/10.1039/c9an01144g.

[50] M. Ji, S. Lewis, S. Camelo-Piragua, S.H. Ramkissoon, M. Snuderl, S. Venneti, A. Fisher-

Hubbard, M. Garrard, D. Fu, A.C. Wang, J.A. Heth, C.O. Maher, N. Sanai, T.D. Johnson, C.W. Freudiger, O. Sagher, X.S. Xie, D.A. Orringer, Detection of human brain tumor infiltration with quantitative stimulated Raman scattering microscopy, Sci. Transl. Med. 7(309) (2015). https://doi.org/10.1126/scitranslmed.aab0195.

[51] F.-K. Lu, D. Calligaris, O.I. Olubiyi, I. Norton, W. Yang, S. Santagata, X.S. Xie, A.J. Golby, N.Y.R. Agar, Label-Free Neurosurgical Pathology with Stimulated Raman Imaging, Cancer Res. 76(12) (2016) 3451-3462. https://doi.org/10.1158/0008-5472.Can-16-0270.

[52] D. Vrazhnov, A. Mankova, E. Stupak, Y. Kistenev, A. Shkurinov, O. Cherkasova, Discovering Glioma Tissue through Its Biomarkers' Detection in Blood by Raman Spectroscopy and Machine Learning, Pharmaceutics 15(1) (2023). https://doi.org/10.3390/pharmaceutics15010203.

[53] T.C. Hollon, B. Pandian, E. Urias, A.V. Save, A.R. Adapa, S. Srinivasan, N.K. Jairath, Z. Farooq, T. Marie, W.N. Al-Holou, K. Eddy, J.A. Heth, S.S.S. Khalsa, K. Conway, O. Sagher, J.N. Bruce, P. Canoll, C.W. Freudiger, S. Camelo-Piragua, H. Lee, D.A. Orringer, Rapid, label-free detection of diffuse glioma recurrence using intraoperative stimulated Raman histology and deep neural networks, Neuro-oncol. 23(1) (2021) 144-155. https://doi.org/10.1093/neuonc/noaa162.

[54] Z. Jin, Q. Yue, W. Duan, A. Sui, B. Zhao, Y. Deng, Y. Zhai, Y. Zhang, T. Sun, G.P. Zhang, L. Han, Y. Mao, J. Yu, X.Y. Zhang, C. Li, Intelligent SERS Navigation System Guiding Brain Tumor Surgery by Intraoperatively Delineating the Metabolic Acidosis, Advanced Science 9(7) (2022). https://doi.org/10.1002/advs.202104935.

[55] J. Wahl, E. Klint, M. Hallbeck, J. Hillman, K. Wårdell, K. Ramser, Impact of preprocessing methods on the Raman spectra of brain tissue, Biomedical Optics Express 13(12) (2022). https://doi.org/10.1364/boe.476507.

[56] T.C. Hollon, D.A. Orringer, An automated tissue-to-diagnosis pipeline using intraoperative stimulated Raman histology and deep learning, Molecular & Cellular Oncology 7(3) (2020). https://doi.org/10.1080/23723556.2020.1736742.

[57] D.A. Orringer, B. Pandian, Y.S. Niknafs, T.C. Hollon, J. Boyle, S. Lewis, M. Garrard, S.L. Hervey-Jumper, H.J.L. Garton, C.O. Maher, J.A. Heth, O. Sagher, D.A. Wilkinson, M. Snuderl, S. Venneti, S.H. Ramkissoon, K.A. McFadden, A. Fisher-Hubbard, A.P. Lieberman, T.D. Johnson, X.S. Xie, J.K. Trautman, C.W. Freudiger, S. Camelo-Piragua, Rapid intraoperative histology of unprocessed surgical specimens via fibre-laser-based stimulated Raman scattering microscopy, Nature Biomedical Engineering 1(2) (2017). https://doi.org/10.1038/s41551-016-0027.

[58] T.C. Hollon, B. Pandian, A.R. Adapa, E. Urias, A.V. Save, S.S.S. Khalsa, D.G. Eichberg, R.S. D'Amico, Z.U. Farooq, S. Lewis, P.D. Petridis, T. Marie, A.H. Shah, H.J.L. Garton, C.O. Maher, J.A. Heth, E.L. McKean, S.E. Sullivan, S.L. Hervey-Jumper, P.G. Patil, B.G. Thompson, O. Sagher, G.M. McKhann, 2nd, R.J. Komotar, M.E. Ivan, M. Snuderl, M.L. Otten, T.D. Johnson, M.B. Sisti, J.N. Bruce, K.M. Muraszko, J. Trautman, C.W. Freudiger, P. Canoll, H. Lee, S. Camelo-Piragua, D.A. Orringer, Near real-time intraoperative brain tumor diagnosis using stimulated Raman histology and deep neural networks, Nat. Med. 26(1) (2020) 52-58. https://doi.org/10.1038/s41591-019-0715-9.

[59] L. Di, D.G. Eichberg, K. Huang, A.H. Shah, A.M. Jamshidi, E.M. Luther, V.M. Lu, R.J. Komotar, M.E. Ivan, S.H. Gultekin, Stimulated Raman Histology for Rapid Intraoperative Diagnosis of Gliomas, World Neurosurgery 150 (2021) e135-e143. https://doi.org/10.1016/j.wneu.2021.02.122.

[60] D.N. Louis, A. Perry, P. Wesseling, D.J. Brat, I.A. Cree, D. Figarella-Branger, C. Hawkins, H.K.

Ng, S.M. Pfister, G. Reifenberger, R. Soffietti, A. von Deimling, D.W. Ellison, The 2021 WHO Classification of Tumors of the Central Nervous System: a summary, Neuro-oncol. 23(8) (2021) 1231-1251. https://doi.org/10.1093/neuonc/noab106.

[61] G. Fürtjes, D. Reinecke, N. von Spreckelsen, A.-K. Meißner, D. Rueß, M. Timmer, C. Freudiger, A. Ion-Margineanu, F. Khalid, K. Watrinet, C. Mawrin, A. Chmyrov, R. Goldbrunner, O. Bruns, V. Neuschmelting, Intraoperative microscopic autofluorescence detection and characterization in brain tumors using stimulated Raman histology and two-photon fluorescence, Frontiers in Oncology 13 (2023). https://doi.org/10.3389/fonc.2023.1146031.

[62] Z. Liu, L. Chen, H. Cheng, J. Ao, J. Xiong, X. Liu, Y. Chen, Y. Mao, M. Ji, Virtual formalin-fixed and paraffin-embedded staining of fresh brain tissue via stimulated Raman CycleGAN model, Science Advances 10(13) (2024). https://doi.org/10.1126/sciadv.adn3426.

[63] K. Klein, G.G. Klamminger, L. Mombaerts, F. Jelke, I.F. Arroteia, R. Slimani, G. Mirizzi, A. Husch, K.B.M. Frauenknecht, M. Mittelbronn, F. Hertel, F.B. Kleine Borgmann, Computational Assessment of Spectral Heterogeneity within Fresh Glioblastoma Tissue Using Raman Spectroscopy and Machine Learning Algorithms, Molecules 29(5) (2024). https://doi.org/10.3390/molecules29050979.

[64] A. Ospanov, I. Romanishkin, T. Savelieva, A. Kosyrkova, S. Shugai, S. Goryaynov, G. Pavlova, I. Pronin, V. Loschenov, Optical Differentiation of Brain Tumors Based on Raman Spectroscopy and Cluster Analysis Methods, Int. J. Mol. Sci. 24(19) (2023). https://doi.org/10.3390/ijms241914432.

[65] T.C. Hollon, S. Lewis, B. Pandian, Y.S. Niknafs, M.R. Garrard, H. Garton, C.O. Maher, K. McFadden, M. Snuderl, A.P. Lieberman, K. Muraszko, S. Camelo-Piragua, D.A. Orringer, Rapid Intraoperative Diagnosis of Pediatric Brain Tumors Using Stimulated Raman Histology, Cancer Res. 78(1) (2018) 278-289. https://doi.org/10.1158/0008-5472.Can-17-1974.

[66] A. Quesnel, N. Coles, C. Angione, P. Dey, T.M. Polvikoski, T.F. Outeiro, M. Islam, A.A. Khundakar, P.S. Filippou, Glycosylation spectral signatures for glioma grade discrimination using Raman spectroscopy, BMC Cancer 23(1) (2023). https://doi.org/10.1186/s12885-023-10588-w.

[67] J. Li, C. Wang, Y. Yao, Y. Zhu, C. Yan, Q. Zhuge, L. Qu, C. Han, Label-free discrimination of glioma brain tumors in different stages by surface enhanced Raman scattering, Talanta 216 (2020). https://doi.org/10.1016/j.talanta.2020.120983.

[68] B. Tołpa, W. Paja, E. Trojnar, K. Łach, A. Gala-Błądzińska, A. Kowal, E. Gumbarewicz, P. Frączek, J. Cebulski, J. Depciuch, FT-Raman spectra in combination with machine learning and multivariate analyses as a diagnostic tool in brain tumors, Nanomedicine: Nanotechnology, Biology and Medicine 57 (2024). https://doi.org/10.1016/j.nano.2024.102737.

[69] V. Ranc, O. Pavlacka, O. Kalita, M. Vaverka, Discrimination of resected glioma tissues using surface enhanced Raman spectroscopy and Au@ZrO2 plasmonic nanosensor, Spectrochimica Acta Part A: Molecular and Biomolecular Spectroscopy 305 (2024). https://doi.org/10.1016/j.saa.2023.123521.

[70] F. Daoust, T. Nguyen, P. Orsini, J. Bismuth, M.-M. de Denus-Baillargeon, I. Veilleux, A. Wetter, P. McKoy, I. Dicaire, M. Massabki, K. Petrecca, F. Leblond, Handheld macroscopic Raman spectroscopy imaging instrument for machine-learning-based molecular tissue margins characterization, J. Biomed. Opt. 26(02) (2021). https://doi.org/10.1117/1.Jbo.26.2.022911.

[71] Q. Yue, X. Gao, Y. Yu, Y. Li, W. Hua, K. Fan, R. Zhang, J. Qian, L. Chen, C. Li, Y. Mao, An EGFRvIII targeted dual-modal gold nanoprobe for imaging-guided brain tumor surgery, Nanoscale 9(23) (2017) 7930-7940. https://doi.org/10.1039/c7nr01077j.

[72] L. Zhang, Y. Zhou, B. Wu, S. Zhang, K. Zhu, C.-H. Liu, X. Yu, R.R. Alfano, A Handheld Visible Resonance Raman Analyzer Used in Intraoperative Detection of Human Glioma, Cancers 15(6) (2023). https://doi.org/10.3390/cancers15061752.

[73] M. Jermyn, K. Mok, J. Mercier, J. Desroches, J. Pichette, K. Saint-Arnaud, L. Bernstein, M.-C. Guiot, K. Petrecca, F. Leblond, Intraoperative brain cancer detection with Raman spectroscopy in humans, Sci. Transl. Med. 7(274) (2015). https://doi.org/10.1126/scitranslmed.aaa2384.

[74] J. Desroches, M. Jermyn, K. Mok, C. Lemieux-Leduc, J. Mercier, K. St-Arnaud, K. Urmey, M.-C. Guiot, E. Marple, K. Petrecca, F. Leblond, Characterization of a Raman spectroscopy probe system for intraoperative brain tissue classification, Biomedical Optics Express 6(7) (2015). https://doi.org/10.1364/boe.6.002380.

[75] L. Han, W. Duan, X. Li, C. Wang, Z. Jin, Y. Zhai, C. Cao, L. Chen, W. Xu, Y. Liu, Y.-Y. Bi, J. Feng, Y. Mao, Q. Yue, X.-Y. Zhang, C. Li, Surface-Enhanced Resonance Raman Scattering-Guided Brain Tumor Surgery Showing Prognostic Benefit in Rat Models, ACS Appl. Mater. Interfaces 11(17) (2019) 15241-15250. https://doi.org/10.1021/acsami.9b00227.

[76] D.N. Louis, H. Ohgaki, O.D. Wiestler, W.K. Cavenee, P.C. Burger, A. Jouvet, B.W. Scheithauer, P. Kleihues, The 2007 WHO Classification of Tumours of the Central Nervous System, Acta Neuropathol. 114(2) (2007) 97-109. https://doi.org/10.1007/s00401-007-0243-4.

[77] D.N. Louis, A. Perry, G. Reifenberger, A. von Deimling, D. Figarella-Branger, W.K. Cavenee, H. Ohgaki, O.D. Wiestler, P. Kleihues, D.W. Ellison, The 2016 World Health Organization Classification of Tumors of the Central Nervous System: a summary, Acta Neuropathol. 131(6) (2016) 803-820. https://doi.org/10.1007/s00401-016-1545-1.

[78] W. Wang, Y. Zhao, L. Teng, J. Yan, Y. Guo, Y. Qiu, Y. Ji, B. Yu, D. Pei, W. Duan, M. Wang, L. Wang, J. Duan, Q. Sun, S. Wang, H. Duan, C. Sun, Y. Guo, L. Luo, Z. Guo, F. Guan, Z. Wang, A. Xing, Z. Liu, H. Zhang, L. Cui, L. Zhang, G. Jiang, D. Yan, X. Liu, H. Zheng, D. Liang, W. Li, Z.-C. Li, Z. Zhang, Neuropathologist-level integrated classification of adult-type diffuse gliomas using deep learning from whole-slide pathological images, Nat. Commun. 14(1) (2023). https://doi.org/10.1038/s41467-023-41195-9.

[79] P. Śledzińska, M.G. Bebyn, J. Furtak, J. Kowalewski, M.A. Lewandowska, Prognostic and Predictive Biomarkers in Gliomas, Int. J. Mol. Sci. 22(19) (2021). https://doi.org/10.3390/ijms221910373.

[80] J.J. Miller, L.N. Gonzalez Castro, S. McBrayer, M. Weller, T. Cloughesy, J. Portnow, O. Andronesi, J.S. Barnholtz-Sloan, B.G. Baumert, M.S. Berger, W.L. Bi, R. Bindra, D.P. Cahill, S.M. Chang, J.F. Costello, C. Horbinski, R.Y. Huang, R.B. Jenkins, K.L. Ligon, I.K. Mellinghoff, L.B. Nabors, M. Platten, D.A. Reardon, D.D. Shi, D. Schiff, W. Wick, H. Yan, A. von Deimling, M. van den Bent, W.G. Kaelin, P.Y. Wen, Isocitrate dehydrogenase (IDH) mutant gliomas: A Society for Neuro-Oncology (SNO) consensus review on diagnosis, management, and future directions, Neuro-oncol. 25(1) (2023) 4-25. https://doi.org/10.1093/neuonc/noac207.

[81] J.J. Miller, Targeting IDH-Mutant Glioma, Neurotherapeutics 19(6) (2022) 1724-1732. https://doi.org/10.1007/s13311-022-01238-3.

[82] Y.S. Choi, S. Bae, J.H. Chang, S.-G. Kang, S.H. Kim, J. Kim, T.H. Rim, S.H. Choi, R. Jain, S.-K. Lee, Fully automated hybrid approach to predict theIDHmutation status of gliomas via deep learning and radiomics, Neuro-oncol. 23(2) (2021) 304-313. https://doi.org/10.1093/neuonc/noaa177.

[83] T.C. Hollon, D.A. Orringer, Shedding Light on IDH1 Mutation in Gliomas, Clin. Cancer Res.

24(11) (2018) 2467-2469. https://doi.org/10.1158/1078-0432.Ccr-18-0011.
[84] K. Bae, W. Zheng, K. Lin, S.W. Lim, Y.K. Chong, C. Tang, N.K. King, C.B. Ti Ang, Z. Huang, Epi-Detected Hyperspectral Stimulated Raman Scattering Microscopy for Label-Free Molecular Subtyping of Glioblastomas, Anal. Chem. 90(17) (2018) 10249-10255. https://doi.org/10.1021/acs.analchem.8b01677.
[85] O. Uckermann, W. Yao, T.A. Juratli, R. Galli, E. Leipnitz, M. Meinhardt, E. Koch, G. Schackert, G. Steiner, M. Kirsch, IDH1 mutation in human glioma induces chemical alterations that are amenable to optical Raman spectroscopy, J. Neurooncol. 139(2) (2018) 261-268. https://doi.org/10.1007/s11060-018-2883-8.
[86] O. Ansorge, C. Vallance, P. Plaha, J. Gannon, J. Walsby-Tickle, C. Scott, I.M. Bell, M. Isabelle, L.J. Livermore, Rapid intraoperative molecular genetic classification of gliomas using Raman spectroscopy, Neuro-Oncology Advances 1(1) (2019). https://doi.org/10.1093/noajnl/vdz008.
[87] T. Sciortino, R. Secoli, E. d'Amico, S. Moccia, M. Conti Nibali, L. Gay, M. Rossi, N. Pecco, A. Castellano, E. De Momi, B. Fernandes, M. Riva, L. Bello, Raman Spectroscopy and Machine Learning for IDH Genotyping of Unprocessed Glioma Biopsies, Cancers 13(16) (2021). https://doi.org/10.3390/cancers13164196.
[88] J. Liu, L. Gao, N. Zhan, P. Xu, J.a. Yang, F.e. Yuan, Y. Xu, Q. Cai, R. Geng, Q. Chen, Hypoxia induced ferritin light chain (FTL) promoted epithelia mesenchymal transition and chemoresistance of glioma, J. Exp. Clin. Cancer Res. 39(1) (2020). https://doi.org/10.1186/s13046-020-01641-8.
[89] A. Golebiewska, A.-C. Hau, A. Oudin, D. Stieber, Y.A. Yabo, V. Baus, V. Barthelemy, E. Klein, S. Bougnaud, O. Keunen, M. Wantz, A. Michelucci, V. Neirinckx, A. Muller, T. Kaoma, P.V. Nazarov, F. Azuaje, A. De Falco, B. Flies, L. Richart, S. Poovathingal, T. Arns, K. Grzyb, A. Mock, C. Herold-Mende, A. Steino, D. Brown, P. May, H. Miletic, T.M. Malta, H. Noushmehr, Y.-J. Kwon, W. Jahn, B. Klink, G. Tanner, L.F. Stead, M. Mittelbronn, A. Skupin, F. Hertel, R. Bjerkvig, S.P. Niclou, Patient-derived organoids and orthotopic xenografts of primary and recurrent gliomas represent relevant patient avatars for precision oncology, Acta Neuropathol. 140(6) (2020) 919-949. https://doi.org/10.1007/s00401-020-02226-7.
[90] Z. Dong, H. Cui, Epigenetic modulation of metabolism in glioblastoma, Semin. Cancer Biol. 57 (2019) 45-51. https://doi.org/10.1016/j.semcancer.2018.09.002.
[91] W. Wick, M. Weller, M. van den Bent, M. Sanson, M. Weiler, A. von Deimling, C. Plass, M. Hegi, M. Platten, G. Reifenberger, MGMT testing—the challenges for biomarker-based glioma treatment, Nature Reviews Neurology 10(7) (2014) 372-385. https://doi.org/10.1038/nrneurol.2014.100.
[92] N. Wang, J. Wang, P. Wang, N. Ji, S. Yue, Label-Free Raman Spectromicroscopy Unravels the Relationship between MGMT Methylation and Intracellular Lipid Accumulation in Glioblastoma, Anal. Chem. 95(31) (2023) 11567-11571. https://doi.org/10.1021/acs.analchem.3c00967.
[93] H.G. Vuong, T.Q. Nguyen, T.N.M. Ngo, H.C. Nguyen, K.-M. Fung, I.F. Dunn, The interaction between TERT promoter mutation and MGMT promoter methylation on overall survival of glioma patients: a meta-analysis, BMC Cancer 20(1) (2020). https://doi.org/10.1186/s12885-020-07364-5.
[94] M.J. van den Bent, C.M.S. Tesileanu, W. Wick, M. Sanson, A.A. Brandes, P.M. Clement, S. Erridge, M.A. Vogelbaum, A.K. Nowak, J.F. Baurain, W.P. Mason, H. Wheeler, O.L. Chinot, S. Gill, M. Griffin, L. Rogers, W. Taal, R. Rudà, M. Weller, C. McBain, J. Reijneveld, R.H. Enting, F.

Caparrotti, T. Lesimple, S. Clenton, A. Gijtenbeek, E. Lim, U. Herrlinger, P. Hau, F. Dhermain, I. de Heer, K. Aldape, R.B. Jenkins, H.J. Dubbink, J.M. Kros, P. Wesseling, S. Nuyens, V. Golfinopoulos, T. Gorlia, P. French, B.G. Baumert, Adjuvant and concurrent temozolomide for 1p/19q non-co-deleted anaplastic glioma (CATNON; EORTC study 26053-22054): second interim analysis of a randomised, open-label, phase 3 study, The Lancet Oncology 22(6) (2021) 813-823. https://doi.org/10.1016/s1470-2045(21)00090-5.

[95] W. Di, W. Fan, F. Wu, Z. Shi, Z. Wang, M. Yu, Y. Zhai, Y. Chang, C. Pan, G. Li, U.D. Kahlert, W. Zhang, Clinical characterization and immunosuppressive regulation of CD161 (KLRB1) in glioma through 916 samples, Cancer Sci. 113(2) (2021) 756-769. https://doi.org/10.1111/cas.15236.

[96] O.R. Tamtaji, M. Behnam, M.A. Pourattar, M.R. Hamblin, M. Mahjoubin-Tehran, H. Mirzaei, Z. Asemi, PIWI-interacting RNAs and PIWI proteins in glioma: molecular pathogenesis and role as biomarkers, Cell Communication and Signaling 18(1) (2020). https://doi.org/10.1186/s12964-020-00657-z.

[97] S. Valtorta, D. Salvatore, P. Rainone, S. Belloli, G. Bertoli, R.M. Moresco, Molecular and Cellular Complexity of Glioma. Focus on Tumour Microenvironment and the Use of Molecular and Imaging Biomarkers to Overcome Treatment Resistance, Int. J. Mol. Sci. 21(16) (2020). https://doi.org/10.3390/ijms21165631.

[98] L. Cheng, H. Wu, X. Zheng, N. Zhang, P. Zhao, R. Wang, Q. Wu, T. Liu, X. Yang, Q. Geng, I. Birol, GPGPS: a robust prognostic gene pair signature of glioma ensembling IDH mutation and 1p/19q co-deletion, Bioinformatics 39(1) (2023). https://doi.org/10.1093/bioinformatics/btac850.

[99] D. Bhattacharya, N. Sinha, J. Saini, Determining chromosomal arms 1p/19q co-deletion status in low graded glioma by cross correlation-periodogram pattern analysis, Scientific Reports 11(1) (2021). https://doi.org/10.1038/s41598-021-03078-1.

[100] A.M. Molinaro, J.W. Taylor, J.K. Wiencke, M.R. Wrensch, Genetic and molecular epidemiology of adult diffuse glioma, Nature Reviews Neurology 15(7) (2019) 405-417. https://doi.org/10.1038/s41582-019-0220-2.

[101] S. Ryall, M. Zapotocky, K. Fukuoka, L. Nobre, A. Guerreiro Stucklin, J. Bennett, R. Siddaway, C. Li, S. Pajovic, A. Arnoldo, P.E. Kowalski, M. Johnson, J. Sheth, A. Lassaletta, R.G. Tatevossian, W. Orisme, I. Qaddoumi, L.F. Surrey, M.M. Li, A.J. Waanders, S. Gilheeney, M. Rosenblum, T. Bale, D.S. Tsang, N. Laperriere, A. Kulkarni, G.M. Ibrahim, J. Drake, P. Dirks, M.D. Taylor, J.T. Rutka, S. Laughlin, M. Shroff, M. Shago, L.-N. Hazrati, C. D'Arcy, V. Ramaswamy, U. Bartels, A. Huang, E. Bouffet, M.A. Karajannis, M. Santi, D.W. Ellison, U. Tabori, C. Hawkins, Integrated Molecular and Clinical Analysis of 1,000 Pediatric Low-Grade Gliomas, Cancer Cell 37(4) (2020) 569-583.e5. https://doi.org/10.1016/j.ccell.2020.03.011.

[102] H. Halilibrahimoğlu, K. Polat, S. Keskin, O. Genç, O. Aslan, E. Öztürk-Işık, C. Yakıcıer, A.E. Danyeli, M.N. Pamir, K. Özduman, A. Dinçer, A. Özcan, AssociatingIDHandTERTMutations in Glioma with Diffusion Anisotropy in Normal-Appearing White Matter, American Journal of Neuroradiology 44(5) (2023) 553-561. https://doi.org/10.3174/ajnr.A7855.

[103] M. Gong, X. Fan, H. Yu, W. Niu, S. Sun, H. Wang, X. Chen, Loss of p53 Concurrent with RAS and TERT Activation Induces Glioma Formation, Mol. Neurobiol. 60(6) (2023) 3452-3463. https://doi.org/10.1007/s12035-023-03288-w.

[104] C.N. Saunders, B. Kinnersley, R. Culliford, A.J. Cornish, P.J. Law, R.S. Houlston, Relationship between genetically determined telomere length and glioma risk, Neuro-oncol. 24(2) (2022) 171-181. https://doi.org/10.1093/neuonc/noab208.

[105] L. Shi, A.A. Fung, A. Zhou, Advances in stimulated Raman scattering imaging for tissues and animals, Quantitative Imaging in Medicine and Surgery 11(3) (2020) 1078-1101. https://doi.org/10.21037/qims-20-712.

[106] K. Hanna, E. Krzoska, A.M. Shaaban, D. Muirhead, R. Abu-Eid, V. Speirs, Raman spectroscopy: current applications in breast cancer diagnosis, challenges and future prospects, Br. J. Cancer 126(8) (2021) 1125-1139. https://doi.org/10.1038/s41416-021-01659-5.

[107] L. Huang, H. Sun, L. Sun, K. Shi, Y. Chen, X. Ren, Y. Ge, D. Jiang, X. Liu, W. Knoll, Q. Zhang, Y. Wang, Rapid, label-free histopathological diagnosis of liver cancer based on Raman spectroscopy and deep learning, Nat. Commun. 14(1) (2023) 48. https://doi.org/10.1038/s41467-022-35696-2.

[108] T. Lilo, C.L.M. Morais, C. Shenton, A. Ray, N. Gurusinghe, Revising Fourier-transform infrared (FT-IR) and Raman spectroscopy towards brain cancer detection, Photodiagnosis and Photodynamic Therapy 38 (2022) 102785. https://doi.org/10.1016/j.pdpdt.2022.102785.

[109] Y. Qi, Y. Liu, J. Luo, Recent application of Raman spectroscopy in tumor diagnosis: from conventional methods to artificial intelligence fusion, PhotoniX 4(1) (2023) 22. https://doi.org/10.1186/s43074-023-00098-0.

[110] C. Li, C. Feng, R. Xu, B. Jiang, L. Li, Y. He, C. Tu, Z. Li, The emerging applications and advancements of Raman spectroscopy in pediatric cancers, Frontiers in Oncology 13 (2023) 1044177. https://doi.org/10.3389/fonc.2023.1044177.

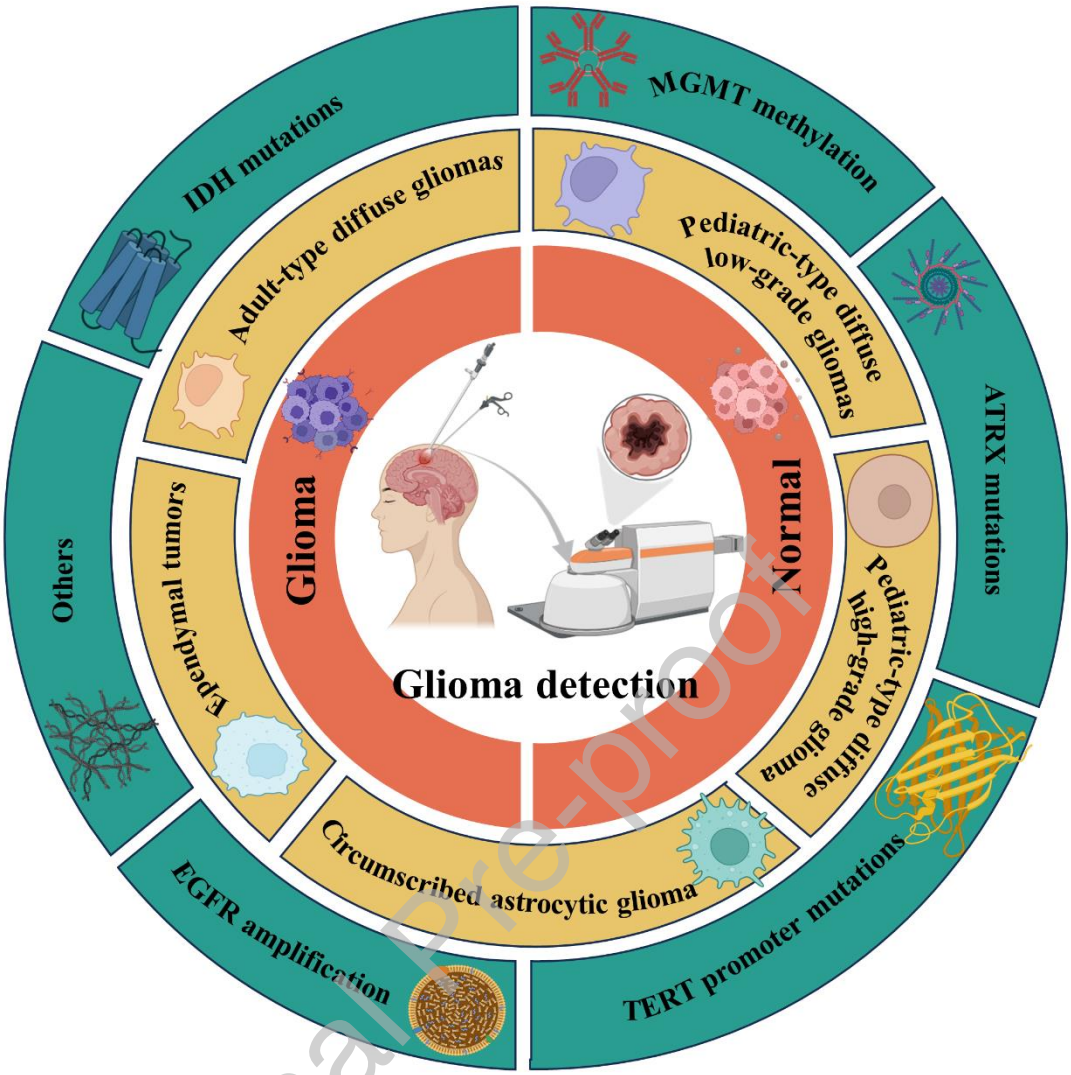

Graphical abstract